CHAPTER NINE: PLATINUM-GROUP MINERALS (PGM), TELLURIDES AND TRACE MINERALS

This chapter documents and compares the PGM assemblages at Nonnenwerth and Townlands, and considers the different processes of formation of these PGM.

A considerable number of platinum group minerals were identified and analysed using a CAMECA SX-100 electron microprobe at the Federal Institute for Geosciences and Natural Resources, Hannover, Germany. Analytical details are given in Appendix 1e and the results are shown in Table 6. The nomenclature followed in this work is that used by Cabri (2002).

The analysed suite of PGM comprises [Pt,Pd]-bismuthotellurides, namely merenskyite [$PdTe_2$], kotulskite [PdTe], moncheite [$PtTe_2$] and michenerite [Pd(Bi,Te)], as well as rare sperrylite [$PtAs_2$] and braggite [(Pd,Pt)S]. Other PGM include isomertieite [$Pd_{11}Sb_2As_2$], stibiopalladinite [Pd_5Sb_2] and temagamite [Pd_3HgTe]. Native gold was also found. Additional minor phases include several tellurides, e.g. tetradymite-type group minerals [Bi_2Te_2S], hessite [Ag_2Te], altaite [PbTe], and pilsenite [Bi_4Te_3]), as well as argento-pentlandite [$Ag(Fe,Ni)_8S_8$] and two unnamed minerals with calculated formulae [Bi_4Te_2Se] and [$FeBiS_2$].

9.1 Nonnenwerth

53 PGM grains were identified at Nonnenwerth. The suite of PGM is dominated by Pd-rich (69 %) and Pt-rich (27 %) bismuthotellurides, as well as one grain each (2 %) of braggite and sperrylite. The PGM occur predominantly at the contact

between sulphide (mostly chalcopyrite, minor pyrrhotite and rare pyrite) and secondary silicate (mostly chlorite and albite after plagioclase), enclosed in silicates or enclosed in sulphides (mostly chalcopyrite and minor pyrrhotite and pyrite). However, even those PGM enclosed in silicates retain a strong spatial relationship with the base metal sulphides, mostly chalcopyrite, and are associated with secondary minerals (mostly chlorite and albite which replace plagioclase, or rarely amphibole which replaces orthopyroxene and base metal sulphides).

Grain sizes of the PGM and other trace minerals range from ca. < 1 µm to 40 µm. The larger grains could thus be readily analysed. Grains < 2 µm in size were analysed qualitatively by energy dispersive spectrometry (EDS).

9.1.1 Recrystallized gabbronorite

The PGM suite (n=34) is dominated by kotulskite [PdTe] (59 %) and moncheite [$PtTe_2$] (35 %). Only one grain each of braggite [(Pd,Pt)S] and sperrylite [$PtAs_2$] were identified. Other trace minerals include hessite [Ag_2Te], native bismuth and a few grains of gold.

Kotulskite [PdTe] occurs enclosed in plagioclase in the vicinity of a chalcopyrite grain (Fig. 9.1a) where it is associated with secondary albite and chlorite, and at chalcopyrite-plagioclase or pyrrhotite-plagioclase grain boundaries. This textural relationship may indicate the partial replacement of chalcopyrite by actinolite (Li *et al.*, 2004). The kotulskite grains occur as clusters of discrete grains often closely associated with moncheite (Fig. 9.1 c to f). In places, kotulskite occurs as composite grains with sperrylite and gold (Fig. 9.1g) or hessite. In the triangular

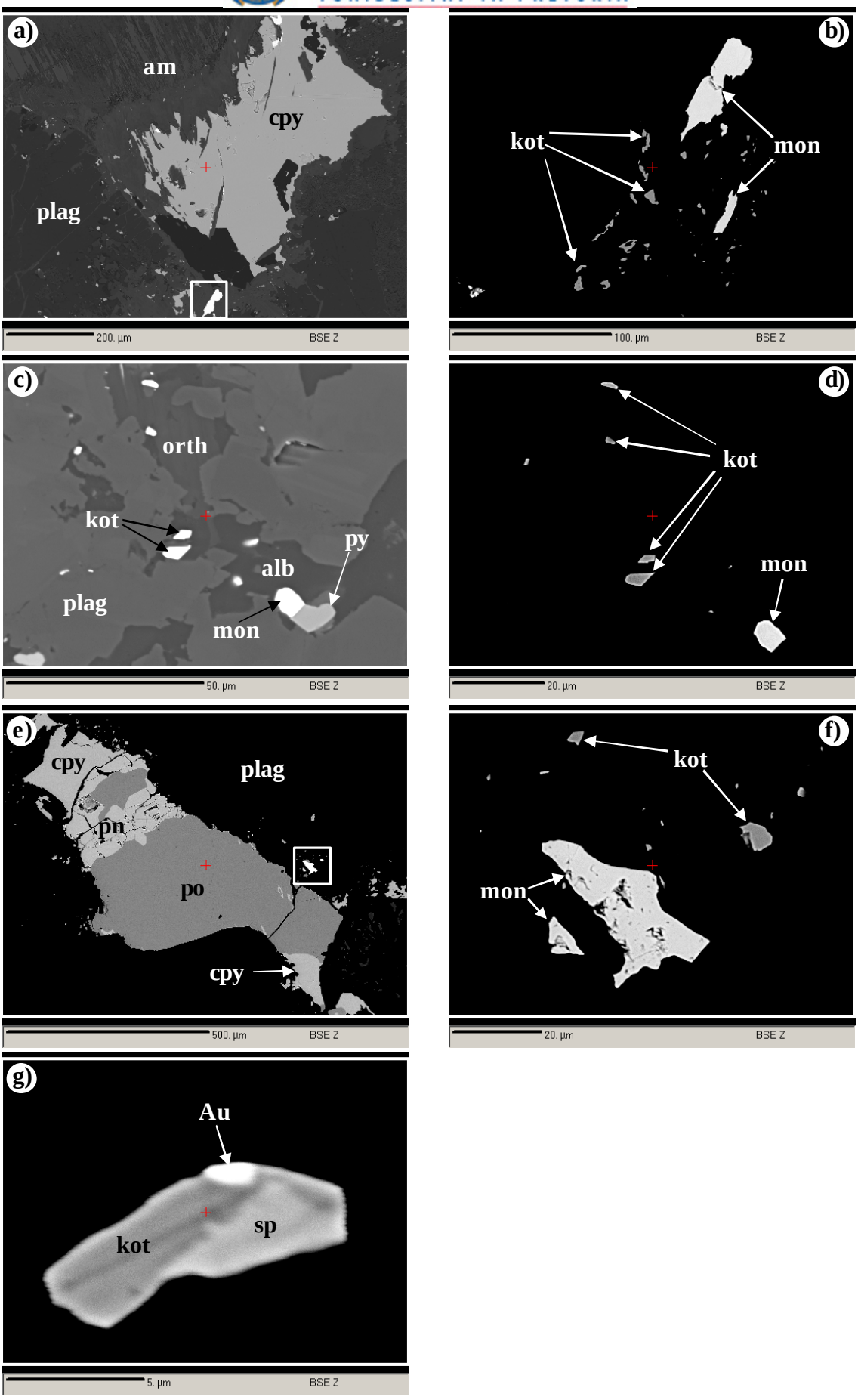

Fig. 9.1: Refer to next page for explanation of the images

plot (Pt+Pd)-(Bi+Sb)-Te for Pd-dominated (Pt,Pd)-bismuthotellurides (i.e., those with Pd > Pt atomic percent; Fig. 9.2a), most of the kotulskite compositions plot along the join kotulskite [PdTe] – sobolevskite [PdBi], suggesting significant substitution of Te by Bi, i.e., kotulskite and sobolevskite form a solid solution. Bismuth contents in kotulskite from recrystallized gabbronorite samples range from 3.84 to 13.98 wt. %.

Moncheite [$PtTe_2$] is euhedral or subhedral with grain sizes ranging from < 5 µm to 40 µm, but mostly between 5 and 20 µm. Like kotulskite, moncheite occurs mostly enclosed in plagioclase, where it is intergrown with secondary minerals (chlorite and amphibole) and generally located close to the edges of plagioclase adjacent to pyrrhotite and chalcopyrite (Fig. 9.1e, f, h & i). This could indicate replacement of sulphides by silicates, resulting in mobility of S, Fe, Cu and formation of PGM

Fig. 9.1:
Back-scattered electron images showing various textures and associations of PGM and gold. Rectangles represent area enlarged in the image to the immediate right.

(a) PGM (in rectangle) enclosed in plagioclase (plag) that has been altered to amphibole (am), in the vicinity of chalcopyrite (cpy). Sample MOX9. (b) Enlarged rectangle from a). Anhedral moncheite (mon) is associated with disseminated anhedral kotulskite (kot) in amphibole (black). Sample MOX9. (c) Kotulskite and moncheite enclosed in altered portions of plagioclase. Moncheite is in contact with pyrite. orth = orthoclase, alb = albite. Sample MOX9. (d) Euhedral to subhedral kotulskite and moncheite. Altered plagioclase is shown in black. Sample MOX9. (e) Composite grain of pyrrhotite (po), pentlandite (pn) and chalcopyrite, with PGM (in rectangle) situated in the periphery of the grain. Sample MOX10. (f) Enlarged rectangle from e). Subhedral to anhedral moncheite and associated kotulskite occur included in altered plagioclase (black background). Sample MOX10. (g) A composite grain of kotulskite, gold (Au) and sperrylite in altered plagioclase (black background). Sample MOX9.

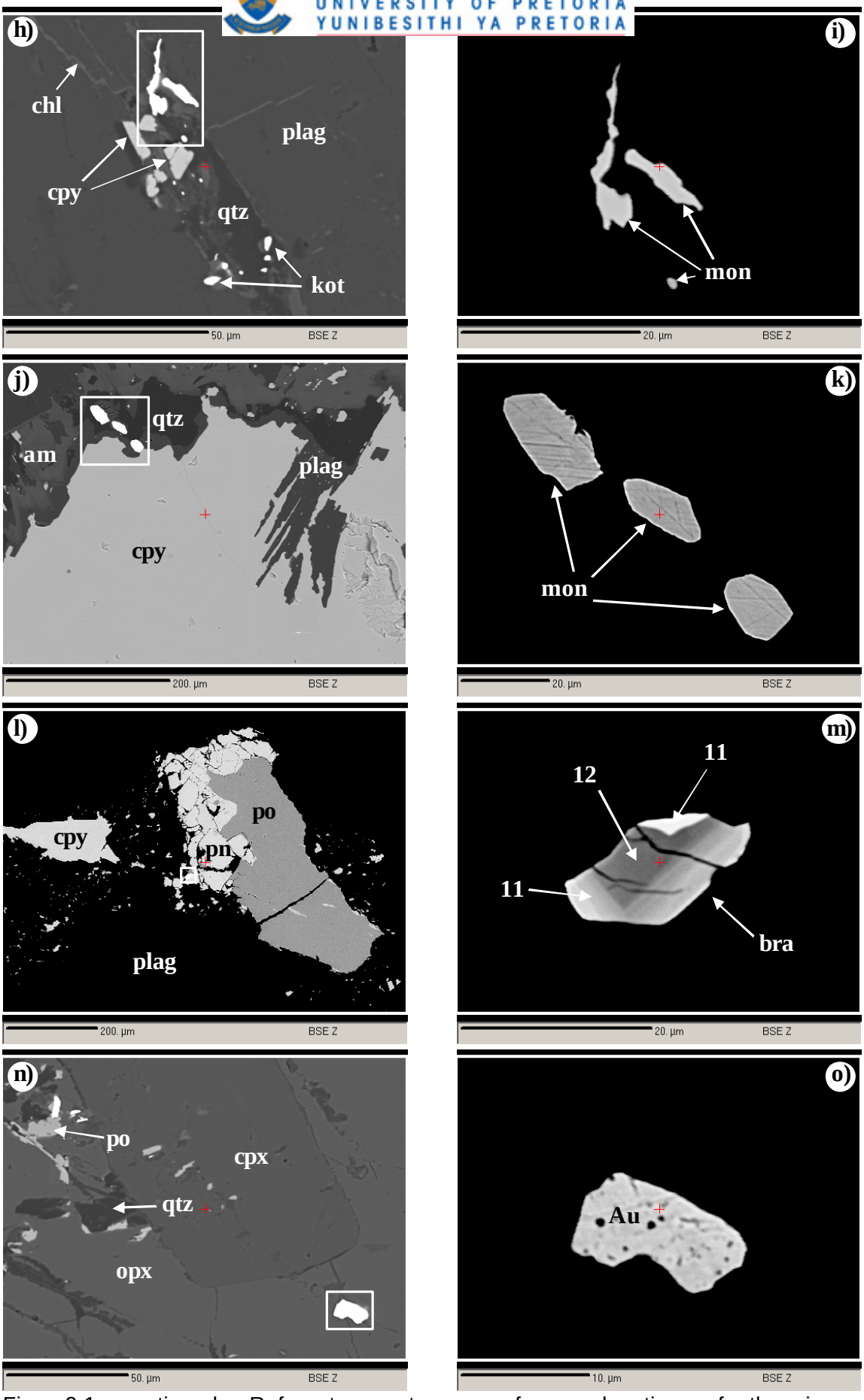

Fig. 9.1 continued: Refer to next page for explanation of the images.

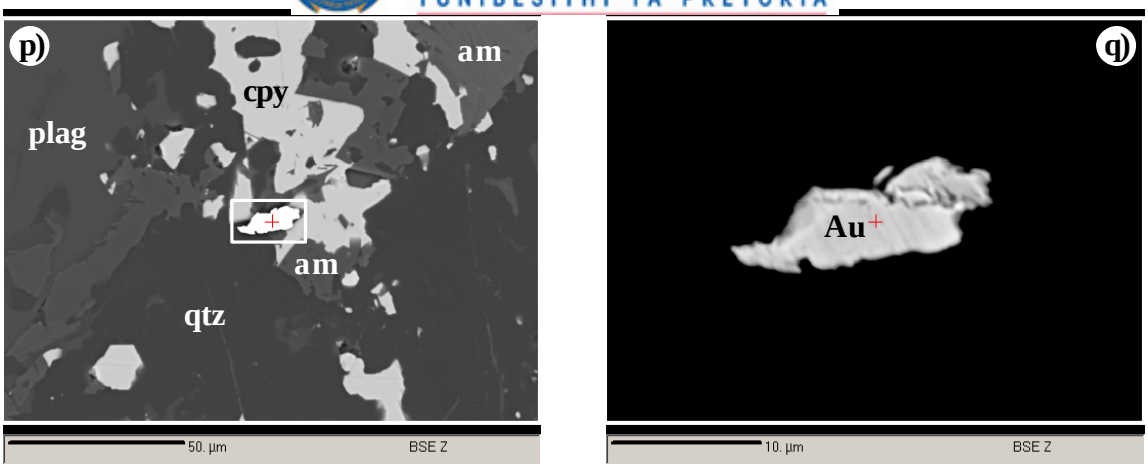

Fig. 9.1 continued:

Fig. 9.1 continued:

Back-scattered electron images showing various textures and associations of PGM and gold. Rectangle represents area enlarged for image to the immediate right.

(h) Chalcopyrite and PGM associated with quartz (qtz) and chlorite (chl), interstitial to plagioclase. Anhedral moncheite is highlighted by rectangle. The other PGM are subhedral kotulskites (kot) Sample MOX9. (i) Enlargement of rectangle from h). Anhedral moncheite is enclosed in chlorite (black background). Sample MOX9. (j) Subhedral moncheite forming a trail from the margin of chalcopyrite (cpy) into adjacent quartz and amphibole (after plagioclase). Sample MOX9. (k) Enlargement of rectangle from j. (l) Intergrown pyrrhotite and pentlandite, with braggite (in rectangle) occurring near margin of sulphide. Sample MOX10. (m) Enlargement of rectangle from l). Zoned subhedral grain of braggite. Increase in brightness corresponds to increase in Pt content. The numbers correspond to analyses e.g. 11 represents 11_MOX10 in Table 6 (Sample MOX10). (n) Grain of gold (Au) (in rectangle) located near fracture in orthopyroxene (opx). Sample MOX12. (o) Enlargement of rectangle from n). Subhedral grain of gold is partly corroded. Sample MOX12. (p) Gold (in rectangle) located at the contact between quartz (qtz) and chalcopyrite (cpy). Sample MOX9. (q) Enlargement of rectangle in p). Sample MOX9.

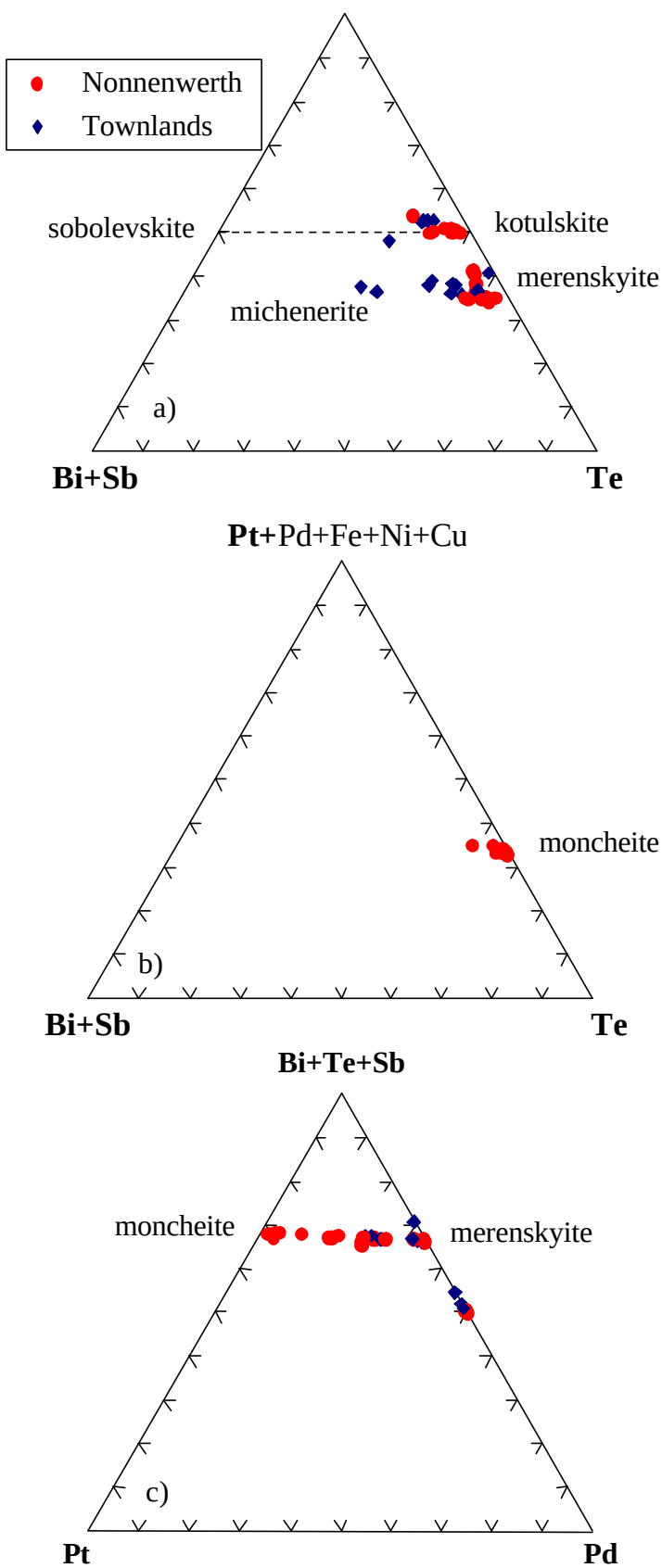

Fig. 9.2: Mineral chemistry of (Pt,Pd)-bismuthotellurides from Nonnenwerth and Townlands. a) Pd-dominated (Pt,Pd)-bismuthotellurides in the triangular plot (Pt+Pd)- (Bi+Sb)-Te (at. %). b) Pt-dominated (Pt,Pd)-bismuthotellurides in the triangular plot (Pd+Pt)-(Bi+Sb)-Te (at. %). c) (Pt,Pd)-bismuthotellurides in the triangular plot (Bi+Te+Sb)-Pt-Pd (at. %).

due to immobility of PGE (Li et al., 2004). In one instance, discrete, euhedral grains of moncheite form a linear trail emanating from the chalcopyrite-plagioclase grain boundary into plagioclase (Fig. 9.1j & k). In rare instances, moncheite may occur intergrown with pyrrhotite enclosed in plagioclase. In a plot of the Pt-dominated (Pt,Pd)-bismuthotellurides (Fig. 9.1b), moncheite analyses plot very close to the Pt+Pd+Fe+Ni+Cu – Te join. This point to only minor substitution of Te by Bi. Most grains have < 2 wt. % Bi; only one grain has a Bi content of 3.8 wt. %.

One grain each of sperrylite [$PtAs_2$] and braggite [(Pd,Pt)S] were identified. Quantitative analyses are given in Table 6a. Sperrylite is ~ 5 µm in size, and occurs as a composite grain with kotulskite and gold (Fig. 9.1g). Braggite is ~ 20 µm in size, of subhedral habit and occurs at the contact between chalcopyrite, pyrrhotite and plagioclase (Fig. 9.1l &m). The grain shows zoning defined by variation in Pd/Pt ratio. In the triangular plot Pt-Pd-Ni (Fig. 9.3), analyses of the braggite grain plot in a line parallel to the Pt-Pd join and show substantial substitution of Pd for Pt with Pd ranging from 10.70 – 31.15 at % and Ni 9.02 – 10.26 at %. The single grain of braggite clearly displays the solid solution between braggite [(Pt,Pd,Ni)S] and vysotskite [PdS] (Verryn and Merkle, 2000).

Seven grains of anhedral and rounded native gold were found in the recrystallized gabbronorite samples. Grain sizes range from < 1 µm to 15 µm. The grains occur enclosed in plagioclase (Fig. 9.1n & o) or along internal fractures in orthopyroxene altered to amphibole in the vicinity of chalcopyrite (Fig. 9.1p & q). The grain enclosed in plagioclase occurs intergrown with kotulskite and hessite. Ag contents

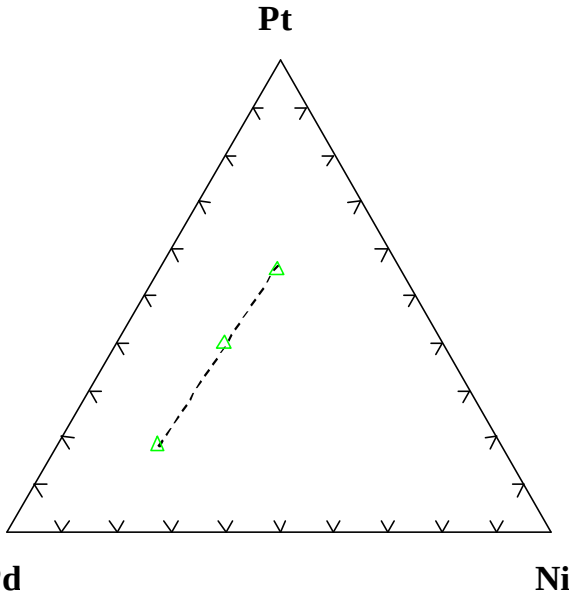

Fig. 9.3: Mineral chemistry of braggite from Nonnenwerth (sample MOX10).

of gold grains range from 12.9 to 20.62 wt. %, with the low Ag bearing gold enclosed in plagioclase. Trace contents of Pd in gold ranges from 0.36 to 0.6 wt. %.

One grain of hessite [Ag_2Te] has been identified and analysed. The grain is ~5 µm in size, and occurs intergrown with kotulskite at the chalcopyrite-plagioclase grain boundary. The chemical composition of the grain is given in Table 6a.

9.1.2 Anorthosite

The PGM suite (n=18) mainly comprises merenskyite (89 %). In addition, one grain each of kotulskite and moncheite were observed. The relative scarcity of moncheite and kotulskite in anorthosite is notable because these minerals dominate the PGM suite in recrystallized gabbronorite.

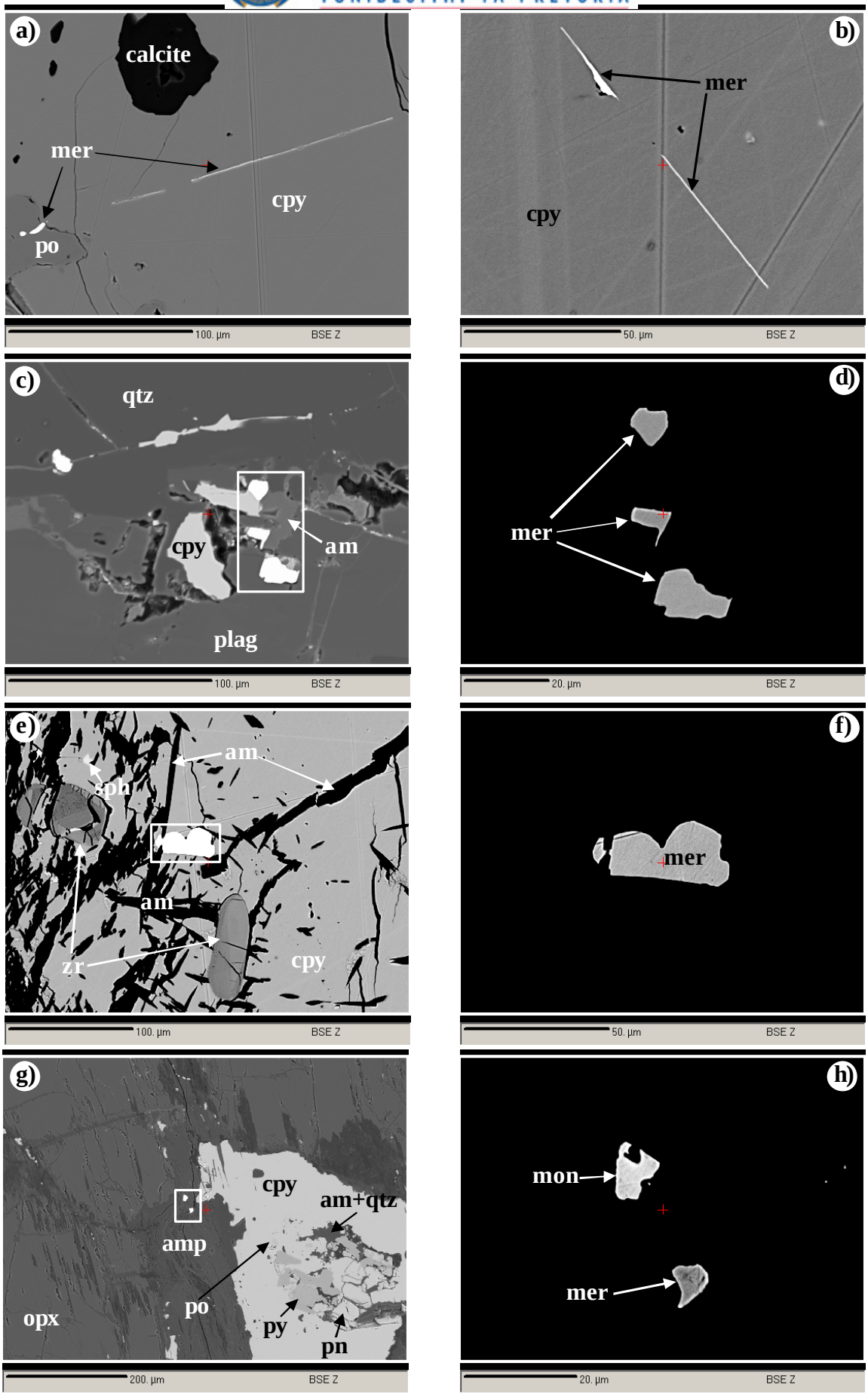

Fig. 9.4: Refer to next page for explanation of images.

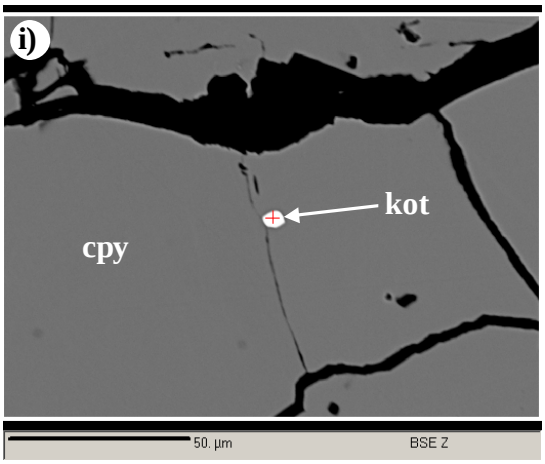

Fig. 9.4: Back-scattered electron images showing various textures and associations of PGM. (a) Merenskyite (mer) enclosed in pyrrhotite (po) and occurring as thin lamellae in chalcopyrite. Note also calcite enclosed in chalcopyrite. Sample MOX29. (b) Merenskyite lamellae in chalcopyrite. Sample MOX29. (c) Merenskyite (in rectangle) intergrown with amphibole, quartz and chalcopyrite within plagioclase. Sample MOX29. (d) Enlargement of rectangle in c). Subhedral merenskyite grains in amphibole and quartz after plagioclase. Sample MOX29. (e) Merenskyite (in rectangle) enclosed in chalcopyrite that is intergrown with acicular amphiboles (actinolite). Chalcopyrite also encloses subhedral zircons (zr). Sample MOX29. (f) Enlargement of rectangle in e). Subhedral merenskyite enclosed in chalcopyrite. Sample MOX29. (g) PGM (in rectangle) in amphibole peripheral to a composite grain of chalcopyrite, pyrrhotite and pentlandite. Sample MOX27. (h) Enlargement of rectangle in g) Anhedral moncheite and merenskyite in amphibole. Sample MOX27. (i) Kotulskite enclosed in chalcopyrite, close to a fracture. Sample MOX29.

Merenskyite [$PdTe_2$] shows grain sizes between < 1 µm to 18 µm, occasionally reaching 50 µm, but mostly around 10 µm. It occurs as lamellae in chalcopyrite (Fig. 9.4a & b) suggesting that it exsolved from the sulphide. It also occurs as subhedral to anhedral grains at the boundary between chalcopyrite and altered plagioclase or enclosed in plagioclase in the vicinity of chalcopyrite (Fig. 9.4c & d). In places, it may occur enclosed in pyrrhotite, pentlandite or chalcopyrite where

the sulphides are intergrown with amphiboles (Fig. 9.4e & f). Bismuth contents vary substantially and range from 2.17 to 14.82 wt. % (Table 6a).

One crystal of moncheite [$PtTe_2$] examined is anhedral, measuring ~12 µm in size and occurs in amphibole adjacent to a large grain of intergrown chalcopyrite-pentlandite-pyrite-pyrrhotite. It is closely associated with merenskyite (Fig. 9.4g & h). The analysed grain has relatively high Bi contents (8.72 wt. %).

The analysed grain of kotulskite [(PdTe] is ~3 µm in size, subrounded and occurs enclosed in chalcopyrite, close to a fracture (Fig. 9.4i). Quantitative analyses of this grain show that it has a relatively high Bi content (17.12 wt. %) when compared to the maximum of 13.98 wt. % in samples from the recrystallized gabbronorite.

One grain of argento-pentlandite (~2 um) intergrown with chalcopyrite was identified. Quantitative analyses of this grain are given in Table 6a.

9.2 Townlands

The PGM assemblage at Townlands is dominated by Pd-rich (75 %) bismuthotellurides, minor sperrylite (15 %), rare stibiopalladinite (5 %) and isomertieite (5 %). The PGM occur predominantly enclosed in sulphides (mostly pyrite and minor chalcopyrite and millerite) or, in places, at the contact between sulphide (mostly pyrite, minor chalcopyrite and rare galena) and secondary silicate (amphibole after orthopyroxene).

9.2.1 Upper Platreef

Only one crystal of isomertieite-I ($Pd_{11}Sb_2As_2$), was identified in the Upper Platreef. The crystal (~8 µm) is subrounded and occurs enclosed in chalcopyrite, near the contact with intergrown pyrite (Fig. 9.5a & b). The chemical composition of the grain is given in Table 6b. In addition to the stoichiometric Pd, As and Sb, isomertieite contains significant amounts of Ag (0.84 at. %).

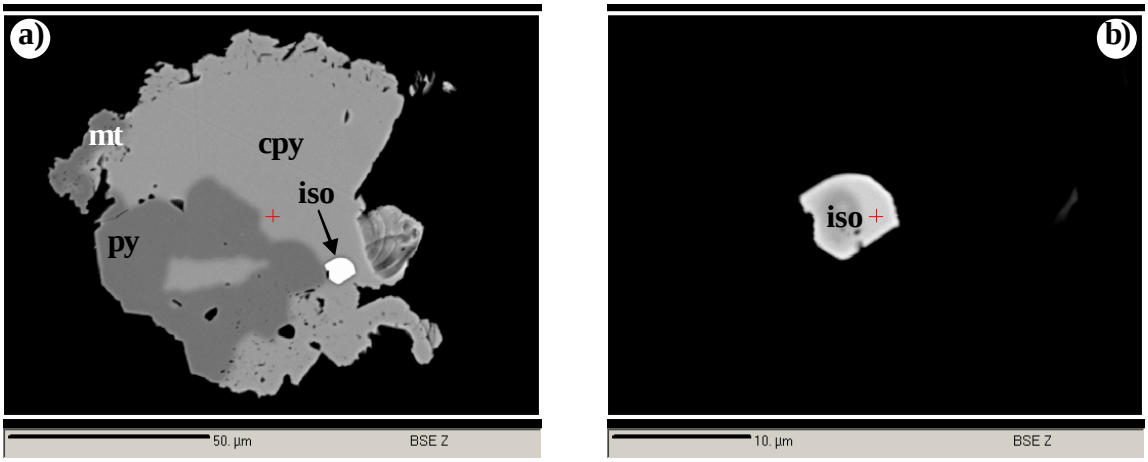

Fig. 9.5: Back-scattered electron images of isomertieite and its textural setting. (a) Isomertieite (iso) enclosed in chalcopyrite, near contact with pyrite. Sample P7. (b) Enlargement of isomertieite shown in a). Sample P7.

9.2.2 Middle Platreef

Compared to the other Platreef packages investigated, the Middle Platreef hosts the largest variety of PGM by far, including PGE-bismuthotellurides, sperrylite, stibiopalladinite as well as Bi-Te phases and gold. In the PGM suite (n=19), Pd-rich bismuthotellurides are predominant (79 %), with lower abundances of sperrylite (16 %) and stibiopalladinite (5 %).

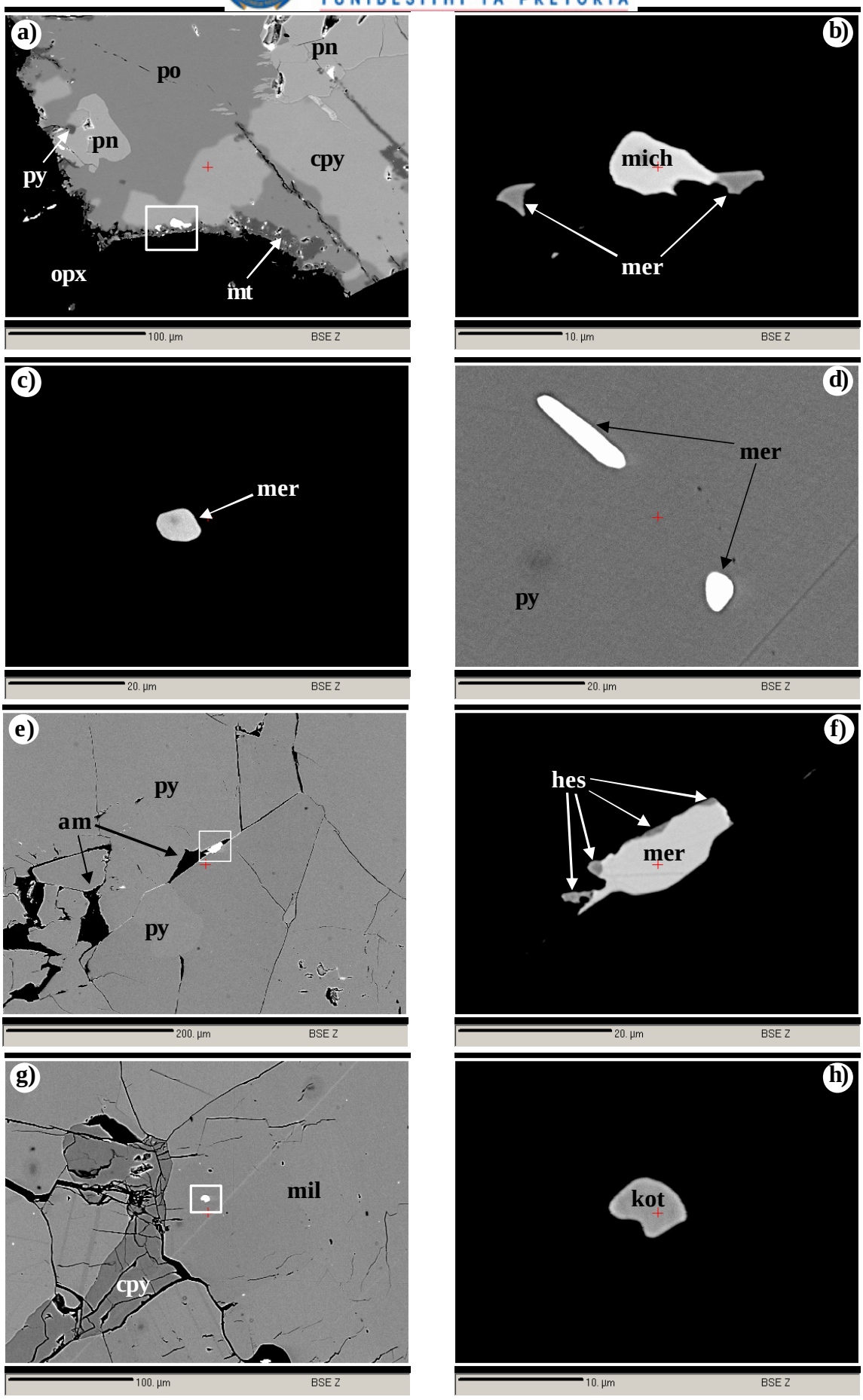

Fig. 9.6: Refer to next page for explanation of the images.

Fig. 9.6: Back-scattered electron images showing various textures and associations of PGM. Rectangle represents area enlarged for image to the immediate right. (a) PGM (in rectangle) enclosed in chalcopyrite (cpy) adjacent to the margin of the sulphide. Magnetite (mt) is also enriched in the border zone of the sulphide. po = pyrrhotite, pn = pentlandite, opx = orthopyroxene. Sample P13. (b) Enlargement of rectangle in a). Subrounded michenerite (mich) intergrown with merenskyite (mer). Sample P13. (c) Subrounded merenskyite enclosed in millerite. Sample P106. (d) A subrounded and an elongate merenskyite grain are enclosed in pyrite (py), associated with a fracture. Sample P15. (e) PGM (in rectangle) enclosed in pyrite along internal cracks. The PGM are associated with amphibole (am) that is intergrown with pyrite, also along cracks. Sample P15. (f) Enlargement of rectangle in e). Anhedral merenskyite intergrown with hessite (hes). Sample P15. (g) Kotulskite (kot) (in rectangle) enclosed in millerite (mil). Note chalcopyrite that is interstitial to millerite. Sample P106. (h) Enlargement of rectangle in g). Subrounded kotulskite enclosed in millerite. Sample P106.

Merenskyite [$PdTe_2$] is subhedral or rounded to elongate in shape with grain sizes ranging from < 2 µm to 22 µm but mostly between 5 and 10 µm. It is enclosed in chalcopyrite and, in general, located close to the margins of chalcopyrite (Fig. 9.6a & b). It may also be enclosed in pyrite (Fig. 9.6c & d) and, in places, in millerite intergrown with pyrite. In one case, several crystals of hessite were observed at the margin of merenskyite (Fig. 9.6e & f). Merenskyite from Townlands is relatively Bi- rich (1.51 to 28.58 wt. %, mostly above 14 wt. %) compared to merenskyite from anorthosite at Nonnenwerth.

Kotulskite [PdTe] occurs enclosed in pyrite, millerite or chalcopyrite (Figs. 9.6g & h). The grains are sub-rounded in shape and grain sizes range from 2 to 7 µm. Quantitative analyses of this phase are given in Table 6b. Three subhedral to anhedral grains of sperrylite [$PtAs_2$] were identified. These occur at pyrrhotite/orthopyroxene grain boundaries (Figs. 9.6i & j). One grain is ~22 µm

wide, the others are < 2 µm in size. Only one quantitative analysis was obtained on the larger grain. In addition to near-stoichiometric Pt and As contents, this grain has 2.14 at. % S, 0.55 at. % Sb, 0.5 at. % Te and 0.1 at. % Rh (Table 6b).

One grain each of michenerite [(Pd,Pt)Te] and stibiopalladinite [Pd_5Sb_2] was identified. The former is subhedral to subrounded, ~10 µm in size, and occurs enclosed in chalcopyrite, close to the margin of the sulphide (Fig. 9.6a & b). The grain is intergrown with merenskyite (Fig. 9.6a & b). Stibiopalladinite is ~1 µm in size of subhedral habit and occurs enclosed in pyrite associated with amphibole.

An unnamed phase with a calculated chemical formula **$FeBiS_2$** was also identified. It probably represents the iron end member of emplectite [$CuBiS_2$] (Wagner and Lorenz, 2002). The mineral occurs enclosed in pyrite and forms subhedral to subrounded and elongate grains with grain sizes up to 15 µm. One grain occurs attached to pyrrhotite, which is enclosed in pyrite (Fig. 9.6k & l). Quantitative analyses of this phase are given in Table 6b.

Hessite [Ag_2Te] occurs enclosed in pyrite, particularly along fractures, where it may be intergrown with amphibole. Grain sizes are < 2 µm. One grain is intergrown with merenskyite and the others form a cluster of discrete grains.

Altaite [PbTe] forms subhedral (≈5 µm), subhedral and anhedral grains that are enclosed in secondary amphibole in the vicinity of coarse base metal sulphides (Fig. 9.6m & n). One of the examined grains is intergrown with galena and the other is intergrown with magnetite (Fig. 9.6m & n).

Tetradymite-type minerals identified have calculated chemical formulae close to [Bi_2Te_2S]. Two identified crystals are subhedral, with grain sizes of 10 and 20 µm, and occur at the boundary between chalcopyrite enclosed in pyrite.

One grain each of pilsenite [Bi_4Te_3], temagamite [Pd_3HgTe_3] and an unnamed phase with a calculated chemical formula $Bi_4Te_2S_2$ were identified. Pilsenite is anhedral to subhedral, < 2 µm in size and occurs enclosed in pyrite, adjacent to chalcopyrite. Temagamite is anhedral, ~2 µm in size and also occurs enclosed in pyrite. Quantitative analyses of these two phases are given in Table 6b.

A small (< 2 µm) grain of an unnamed phase with a calculated formula Bi_4Te_2Se (close to UN 1133; Xiang-ping Gu et a., 2001) was identified. The unnamed phase occurs at the contact between pyrite and pyrrhotite and forms part of a complex composite sulphide enclosed in pyrite consisting of chalcopyrite, pyrrhotite, pilsenite, Fe-emplectite? and the unnamed phase [Bi_4Te_2Se] (Fig. 9.6l).

Three grains of gold enclosed in pyrite were identified. They occur associated with amphibole intergrown with pyrite, or along the contact between pyrite and chalcopyrite (Fig. 9.6o & p). One quantitative analyses was obtained, showing has 67.06 wt. % Au, 30.53 wt. % Ag, 0.11 wt. % Fe and 240 ppm Bi.

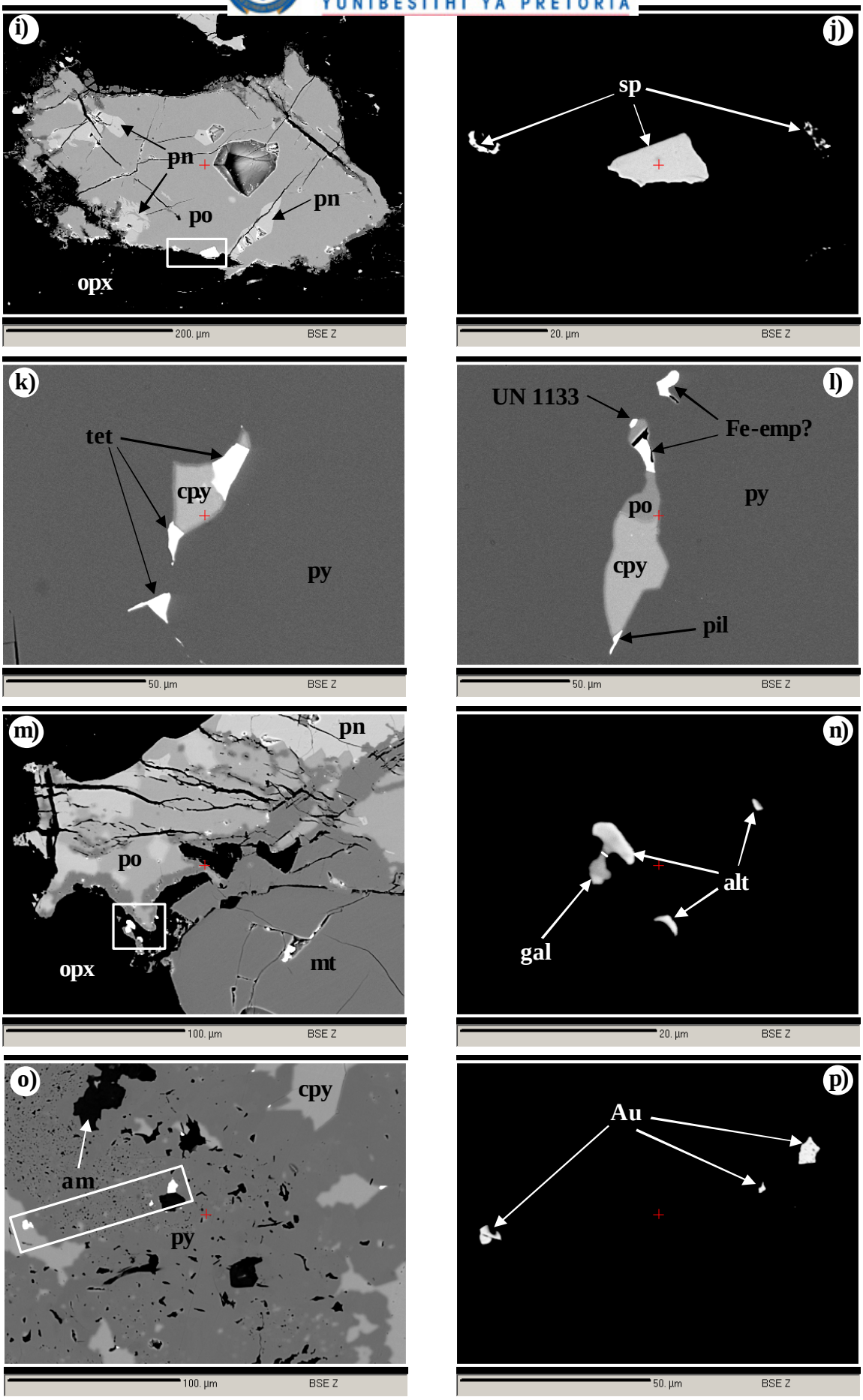

Fig. 9.6 continued: Refer to next page for explanation of the images.

Fig. 9.6 continued: Back scattered electron images showing various textures and associations of PGM and Bi-,Te- phases. Rectangle represents area enlarged for image to the immediate right.

(i) Sperrylite (sp) (in rectangle) located at the contact between pyrrhotite and orthopyroxene (opx). Pyrrhotite is intergrown with pentlandite and also contains minor flame-like exsolutions of pentlandite. Sample P13. (j) Enlargement of rectangle in c). Subhedral sperrylite and smaller anhedral sperrylite at the contact between pyrrhotite and orthopyroxene. Sample P13. (k) Pyrite enclosing intergrowths of tetradymite-type (tet) minerals and chalcopyrite. Sample P15. (l) Pyrite enclosing a composite grain of chalcopyrite, pyrrhotite, pilsenite (pil), Fe-emplectite? (Fe-emp?) and the unnamed phase UN 1133 with a calculated chemical formula [Bi_4Te_2Se]. Sample P15. (m) Altaite (alt) grains (in rectangle) are enclosed in secondary amphibole adjacent to pyrrhotite showing rims of magnetite. Sample P13. (n) Enlargement of rectangle in m). One grain of altaite is intergrown with galena (gal). Sample P13. (o) Gold (Au) grains (in rectangle) enclosed in pyrite or located near the contact between pyrite and enclosed chalcopyrite. Sample P106. (p) Enlargement of rectangle in o). Anhedral gold grains in pyrite. Sample P106.

9.3 Summary and Discussion

At Nonnenwerth, PGM are dominated by **Pd-rich *and* Pt-rich** bismuthotellurides followed by rare braggite and sperrylite. The PGM occur predominantly at the contact between sulphide (mostly chalcopyrite, minor pyrrhotite and rare pyrite) and secondary silicate (mostly chlorite and albite after plagioclase) or enclosed in sulphides. Importantly, Pd-rich PGM (Pd-bismuthotellurides) are mostly enclosed in silicates. However, even these PGM enclosed in silicates retain a strong spatial relationship with the base metal sulphides, mostly chalcopyrite, and are associated with secondary minerals (mostly chlorite and albite which replace plagioclase, or rarely amphibole which replaces orthopyroxene and base metal sulphides). The above observation may result from dissolution of the base metal sulphides hosting Pd, and leaving isolated insoluble Pd-PGM behind (Barnes *et al*., 2007), or Pd

may have been remobilized from the sulphides into the surrounding silicates. Based on textural evidence, the latter model is preferred.

At Townlands, the PGM assemblage is dominated by **Pd-rich** bismuthotellurides, minor sperrylite, rare stibiopalladinite and isomertieite. The PGM occur predominantly enclosed in sulphides (mostly pyrite and minor chalcopyrite and millerite), or locally at the contact between sulphide and secondary silicate (amphibole after orthopyroxene).

In summary, there are no dramatic differences between the PGM assemblages at Nonnenwerth and Townlands, also in comparison to descriptions from most other Platreef occurrences (e.g. Kinloch, 1982; Holwell et al., 2006). Bismuthotellurides predominate followed by rarer arsenides and antimonides. One obvious difference, however, is the wide compositional range of Pt-Pd bismuthotellurides and the presence of Pt-rich bismuthotellurides at Nonnenwerth only, whereas at Townlands, only Pd-rich bismuthotellurides are present. The significance of this finding cannot be evaluated conclusively. The variability may be related to local factors like different host rocks; footwall lithologies, down-temperature re-equilibration, activity of fluids, and other possible causes.

It is here suggested that originally, at magmatic conditions, the PGE were collected by and partitioned into an immiscible sulphide liquid (e.g Naldrett et al., 1986; Naldrett, 1989). The IPGE (Ru, Os, Ir) tend to concentrate into chromite (Lee, 1996), and the PPGE (Pt, Pd and Rh) are mainly concentrated in the sulphide fraction (Naldrett, 1989). During down-temperature crystallisation of the

magmatic sulphide liquid, pyrrhotite, pentlandite and chalcopyrite form on further cooling (Hawley, 1965; Kullerud et al., 1968; Ewers and Hudson, 1972). The PGE are either kept in solid solution in the sulfides (e.g. up to some hundred ppm of Pd in pentlandite at Nonnenwerth; see also Gervilla et al., 2005), or if incompatible with sulfide at lower temperature, PGE-compounds (PGM) are formed by reactions of the PGE with respective ligands like sulphur, arsenic, antimony, tellurium or bismuth. Accordingly, as proposed by Cawthorn et al. (2002), the primary mechanism concentrating the PGE is a first-order process (PGE collection by sulfides), and the evolution of the PGM is the result of secondary processes related to cooling, local changes in $f(S_2)$ in the crystallization environment, subsolidus re-equilibration, and probably also reactions with fluids (late-magmatic to hydrothermal) percolating in the rocks.

The remobilization and redistribution PGE may be attributed to various factors among them assimilation of crustal S where floor rocks are of Transvaal Supergroup, devolatization of dolomite xenoliths which are present along the whole strike length of the northern lobe or interaction of primary magmatic sulphides with late stage magmatic fluids. The involvement of late magmatic/hydrothermal fluids is supported by the occurrence of violarite which is probably of hydrothermal origin.

Addition of floor rock crustal S is supported by the studies of Manyeruke *et al*. (2005). The PGM are dominated by lower temperature Pd-rich bismuthotellurides and minor Bi-, Sb- and Te-bearing phases (Kim et al., 1990), as opposed to the Merensky Reef, where PGE sulphides may constitute a substantial proportion of

the overall PGM assemblage (e.g. Kinloch, 1982; Mostert et al., 1982). Therefore, the PGM assemblages at Nonnenwerth and Townlands support the suggestion that the PGM are “secondary” in the sense of Cawthorn et al. (2002).

The model of sulphide control for the PGE is supported by the broad positive correlation between Pt and Pd and between PGE and S, and abundance of magmatic sulphides at Nonnenwerth suggesting that sulphides were the primary PGE collector. Even though the base metal sulphides do not host the PPGE (Pt, Pd and Rh) – except for a certain proportion of Pd in pentlandite – the PGM that do host them maintain a close spatial relationship with the base metal sulphides, underlining the initial control of PGE by sulphides.

Thus, assimilation of external S during magma emplacement was apparently not the principal controlling factor in sulphide genesis since PGE mineralisation occur at Nonnenwerth where the Platreef over granite gneiss. Instead, significant assimilation of S may have merely modified already existing sulphide melt, essentially diluting the tenor of the sulphides, particularly in areas where the floor rocks consisted of sulphidic shales, between Townlands and Tweefontein (Manyeruke *et al.*, 2005; Hutchinson and Kinnaird, 2005) and the formation of the lower temperature semi-metal PGM e.g. (Pt,Pd)-bismuthotellurides.